

Analysis of a quantum nondemolition measurement scheme based on Kerr nonlinearity in photonic crystal waveguides

Ilya Fushman and Jelena Vučković

Applied Physics, Stanford University

ifushman@stanford.edu

Abstract: We discuss the feasibility of a quantum nondemolition measurement (QND) of photon number based on cross phase modulation due to the Kerr effect in photonic crystal waveguides (PCW's). In particular, we derive the equations for two modes propagating in PCW's and their coupling by a third order nonlinearity. The reduced group velocity and small cross-sectional area of the PCW lead to an enhancement of the interaction relative to bulk materials. We show that in principle, such experiments may be feasible with current photonic technologies, although they are limited by material properties. Our analysis of the propagation equations is sufficiently general to be applicable to the study of soliton formation, all-optical switching and can be extended to processes involving other orders of the nonlinearity.

© 2007 Optical Society of America

OCIS codes: (270.0270) Quantum Optics. (270.5570) Quantum Detectors. (190.0190) Non-linear Optics. (190.4360) Nonlinear Devices. (230.7370) Waveguides

References and links

1. N. Imoto, H. Haus, and Y. Yamamoto, "Quantum nondemolition measurement of the photon number via the optical Kerr effect," *Phys. Rev. A* **32**, 2287 (1985).
2. M.D. Levenson, R.M. Shelby, M. Reid, and D.F. Walls, "Quantum nondemolition Detection of Optical Quadrature Amplitudes," *Phys. Rev. Lett.* **57**, 2473 (1986).
3. S.R. Friberg, S. Machida, and Y. Yamamoto, "Quantum-nondemolition measurement of the photon number of an optical soliton," *Phys. Rev. Lett.* **69**, 3165 (1992).
4. S.R. Friberg, T. Mukai, and S. Machida, "Dual Quantum Nondemolition Measurements via Successive Soliton Collisions," *Phys. Rev. Lett.* **84**, 59 (2000).
5. F. König, B. Buchler, T. Rechtenwald, G. Leuchs, and A. Sitzmann, "Soliton backaction-evading measurement using spectral filtering," *Phys. Rev. A* **66**, 043810 (2002).
6. J.M. Courty, S. Spa, F. König, A. Sitzmann, and G. Leuchs, "Noise-free quantum-nondemolition measurement using optical solitons," *Phys. Rev. A* **58**, 1501 (1998).
7. D. Englund, D. Fattal, E. Waks, G. Solomon, B. Zhang, T. Nakaoka, Y. Arakawa, Y. Yamamoto, and J. Vučković, "Controlling the Spontaneous Emission Rate of Single Quantum Dots in a 2D Photonic Crystal," *Phys. Rev. Lett.* **95**, 013904 (2005).
8. R. W. Boyd, *Nonlinear Optics* (Academic Press, 1991).
9. J. S. Aitchison, D. C. Hutchings, J. U. Kang, G. I. Stegeman, and A. Villeneuve, "The Nonlinear Optical Properties of AlGaAs at the Half Band Gap," *IEEE J. Quantum Electron.* **33**(3), 341 (1997).
10. S. Hoa, C. Socolich, M. Islam, W. Hobson, A. Levi, and R. Slusher, "Large nonlinear phase shifts in low-loss AlGaAs waveguides near half-gap," *Appl. Phys. Lett.* **59**, 2558 (1991).
11. K. Nakatsuhara, T. Mizumoto, E. Takahashi, S. Hossain, Y. Saka, B.-J. Ma, and Y. Nakano, "All-optical switching in a distributed-feedback GaInAsP waveguide," *Appl. Opt.* **38**, 3911 (1999).

12. Y. Yamamoto and A. Imamoglu, *Mesoscopic Quantum Optics* (John Wiley and Sons Inc., 1999).
13. H. Altug and J. Vuckovic, "Experimental demonstration of the slow group velocity of light in two-dimensional coupled photonic crystal microcavity arrays," *Appl. Phys. Lett.* **86**, 111,102 (2005).
14. Y. Vlasov, M. OBoyle, H. Hamann, and S. J. McNab, "Active control of slow light on a chip with photonic crystal waveguides," *Nature* **438**, 66 (2005).
15. J. D. Jackson, *Classical Electrodynamics* (John Wiley and Sons Inc., 1998).
16. M. Settle, M. Salib, A. Michaeli, and T. F. Krauss, "Low loss silicon on insulator photonic crystal waveguides made by 193nm optical lithography," *Opt. Express* **14**., 2440 (2006).
17. A. Villeneuve, C. Yang, G. Stegeman, C. Lin, and H. Lin, "Nonlinear refractive-index and two photon-absorption near half the band gap in AlGaAs," *Appl. Phys. Lett.* **62**, 2465 (1993).
18. E. Waks and J. Vuckovic, "Dispersive properties and giant Kerr non-linearities in Dipole Induced Transparency," *quant-ph/0511205* (2005).
19. K. Nemoto and W. J. Munro, "Nearly Deterministic Linear Optical Controlled-NOT Gate," *Phys. Rev. Lett.* **93**, 250,502 (2004).

1. Introduction

In this paper we focus on the feasibility of realizing the QND photon number measurement proposed in [1] in photonic crystal waveguides (PCW's). QND measurements are important in a variety of quantum information processing techniques as well as quantum state preparation. Although our investigation was motivated by quantum information processing in photonic crystal (PhC) on-chip networks, a detector with the necessary sensitivity may prove to be valuable on its own. The proposed structure can also be employed as a classical photodetector with improved sensitivity. We show that the reduction of group velocity and small interaction volumes in PCWs lead to an effective enhancement of the third order nonlinearity and, theoretically, make QND experiments with high quality structures and attainable laser power levels feasible. We note that QND measurements based on Kerr nonlinearities have been performed and are given in references [2, 3, 4, 5, 6]. These experiments relied on several nonlinear effects in optical fibers including four wave mixing [2] and soliton collision [3, 4, 5, 6]. Soliton collision is the closest to the scheme analyzed in this paper and the equations considered in this work can be extended to studying the formation of solitons in PCW's. Major impediments to the realization of QND measurements in fibers have been parasitic effects such as Brillouin scattering, Raman scattering, self phase modulation, fiber loss etc. Some of these effects can be cleverly circumvented [6]. These effects will most likely be very important for such measurements in PCW's, and have to be analyzed experimentally. The major loss considered here is that due to two photon absorption of the probe pulse, which is not a major loss in optical fibers, but seems to become very important for semiconductor waveguides.

We consider the case of a signal pulse from both a photon number emitter and a coherent state. A typical single photon source is an InGaAs quantum dot (QD) coupled to a PhC cavity as in [7]. The radiative lifetime of such QD's coupled to PhC cavities is $\approx 0.2 - 1ns$. In this experiment, a weak signal pulse is combined with a strong coherent probe in one arm of a Michaelson interferometer. The probe acquires a phase shift that is directly proportional to the signal photon number, and the signal pulse is retained for further use. The main impediment to this measurement is the small value of the nonlinearity and the relatively large photon absorption in semiconductor materials.

The Kerr effect is a third order nonlinearity ($\chi^{(3)}$) and can be described by a weak intensity dependent refractive index (n_2I) as $3\chi^{(3)} = cn^2n_2$, where c is the speed of light and n is the refractive index of the material and I is the Electric field intensity [8]. We will focus on Aluminum Gallium Arsenide (AlGaAs), which has a reasonable $\chi^{(3)}$ and $n_2 \approx 1.510^{-13} \frac{cm^2}{W}$ at a wavelength of 1500 nm and a high refractive index $n \approx 3.4$ [9, 10]. The large refractive index is attractive for the fabrication of PhC devices and can be combined with our current QD sources. Another material system of interest is Indium Gallium Arsenide Phosphide (InGaAsP), which

has $n_2 \approx -5.9 \times 10^{-12} \frac{\text{cm}^2}{\text{W}}$ at 1545 nm [11]. An order of magnitude estimate of the phase due to the nonlinearity can be gained by expanding the index as: $\tilde{n} \approx n + n_2 I$. The relative dielectric constant to first order in intensity is then $\epsilon \approx n^2 + 2nn_2 I$, and the wave vector (k) in the bulk material becomes $k = k_0 + \Delta k = \frac{\omega}{c} \sqrt{\epsilon}$. The acquired phase over a distance L for a signal and probe photons with wavelength λ_s, λ_p and N_s signal photons, is then $\frac{4\pi^2 c \hbar n_2}{\lambda_s \lambda_p \tau_s A} N_s$, which for an area of $A = 1 \mu\text{m}^2$, length $L = 100 \mu\text{m}$, a lifetime of $\tau_s = 1 \text{ns}$ and $\lambda_{p,s} \approx 1.5 \mu\text{m}$ gives $\Delta\Phi \approx 8 \times 10^{-13} \times N_s$. The sensitivity of the interferometer is given by its signal to noise ratio (SNR). The noise in interferometry with coherent states comes from the photon partition noise (shot noise) at the input beamsplitters of the interferometer. It can be shown that in the case of a coherent probe and signal in a number state, the SNR is $(4\phi_s^2 N_p)^{-1}$, where N_p is the probe average photon number, and ϕ_s is the phase due to a single signal photon [12]. This means that $N_p > 10^{23}$ probe photons are needed for the bulk experiment in order to overcome the shot noise when the probe is in a coherent state and the signal is in a number state. This requires a source that can produce a 48kJ pulse with a nanosecond width.

PCW's offer two improvements for such a measurement. First, the group velocity of the pulse propagating in a PhC waveguide is reduced to $v \approx 10^{-2} - 10^{-3} \times c$ [13, 14], and the local intensity increases by this factor. The effective propagation length of the waveguide increases as well, although the losses associated with material absorption and scattering should also increase with the longer effective length. This enhancement merely allows us to make smaller structures. Pulse contraction also means that longer probe pulses can be generated by the external pulse, and will shrink to the desired width. Secondly, the area of the PhC waveguide is of order $\left(\frac{\lambda}{n}\right)^2$.

A combination of these effects leads to an overall enhancement of $\left(\frac{c}{v_g}\right)^2 \frac{A_{\text{bulk}}}{A_{\text{PhC}}} \approx 2 \times 10^5$, for a PhC area of $(250 \text{nm})^2$ and $\frac{v}{c} = 100$. This reduces the energy requirement to $\approx 10^{-6} \text{J}$ in a nanosecond pulse. This figure does not take into account material absorption and waveguide scattering losses, which are generally the main obstacle to such a measurement. We show that with material absorption parameters found in literature and the probe at wavelengths above the half-bandgap of the semiconductors, the experiments could be attempted in a PhC device. Our analysis of the propagation equations is sufficiently general to be applicable to the study of soliton formation, all-optical switching and can be extended to processes involving other orders of the nonlinearity.

In the theoretical proposal, the probe is sent through two arms of a Michaelson interferometer and interacts with the signal in one arm. The phase shift on the probe is measured on the slope of the fringe via homodyne detection [1]. In our case, the interferometer would be made in a free standing membrane of AlGaAs that is patterned by a hexagonal lattice of air holes. The waveguides are made by removing rows of holes. Fig. 1 shows a PCW in a hexagonal lattice and the PCW dispersion for two modes. The group velocity is significantly reduced at the band edge ($k_x = \frac{\pi}{a}$), which makes this an attractive operating point. Numerical precision allows us to estimate that $v_g < c \times 10^{-3}$. Since the Kerr effect depends on the intensity overlap, either two spectrally different points on the same PCW band, or on different bands can be chosen. In the first case, the intensity overlap is maximized, but there is a potential for a large group velocity mismatch. In the second case the mode overlap is sacrificed in favor of matching the group velocities. In principle, $\frac{\Delta\omega}{\omega} \approx 10^{-6}$ for a 1ns pulse, which means that points with very close $\frac{a}{\lambda}$ values can be chosen, and the proximity is limited by the ability to filter, or by the wavelength requirements for the pulse and probe.

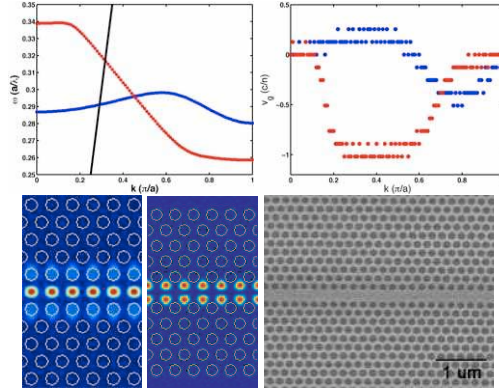


Fig. 1. Top left: waveguide mode dispersions calculated by the 3D Finite Difference Time Domain (FDTD) method. The solid (black) line is the light line in the photonic crystal, above which modes are not confined by total internal reflection. Top right: group velocities of the two modes derived from the dispersion curves by numerical differentiation ($v_g = \frac{d\omega}{dk}$). Bottom left: modes of the PhC lattice at the $k = \frac{\pi}{a}$ point. The mode with even vertical symmetry relative to the waveguide axis corresponds to the red dispersion curve and the odd symmetry mode is that of the blue dispersion curve. Bottom right: A scanning electron micrograph of a fabricated PCW in AlGaAs.

2. Pulse Propagation in PhC Waveguides

First, we derive the equations of motion for the signal and probe pulse in the interferometer. The eigenstates of the PhC waveguide are solutions to:

$$\nabla \times \nabla \times \vec{E} = -\frac{1}{c^2} \frac{\partial^2 (\epsilon(\vec{r}) \vec{E})}{\partial t^2} \quad (1)$$

where $\epsilon(\vec{r})$ is the relative spatially varying waveguide dielectric constant. The solutions are Bloch modes $u_k^m(\vec{r}) e^{i(kz - \omega(k)t)}$ where $u_k^m(\vec{r} + az) = u_k^m(\vec{r})$ for the lattice with periodicity a , z is the direction of propagation along the waveguide, and m is the index of the band of particular symmetry. These modes satisfy the wave equation:

$$\nabla \times \nabla \times (u_k(\vec{r}) e^{ikz}) = \frac{\omega(k)^2}{c^2} \epsilon(\vec{r}) u_k(\vec{r}) e^{ikz} \quad (2)$$

The Bloch state is re-normalized for convenience in the last part of the paper. The waveguide modes can be shown to obey the following orthogonality conditions :

$$\int_{\Omega} d^3 r \epsilon(\vec{r}) u_k^m u_{k'}^n e^{i(k-k')z} = \delta_{mn} \delta_{kk'} \quad (3)$$

where the integral is taken over the whole space Ω . In what follows, index m is dropped, unless it is necessary, and $\epsilon = \epsilon(r)$. The waveguide modes can be rewritten to solve a different Hermitian operator:

$$\hat{O} = \frac{1}{\sqrt{\epsilon}} \nabla \times \nabla \times \frac{1}{\sqrt{\epsilon}} \quad (4)$$

The eigenstates of this operator are $\langle r | u, m, k \rangle = \sqrt{\epsilon} u_k^m(\vec{r}) e^{i(kz - \omega(k)t)}$ with eigenvalue $\frac{\omega(k)^2}{c^2}$, and $\langle u, m, k | u, n, l \rangle = \delta_{m,n} \delta_{k,l}$ by Eq. 3. The inner product denotes integration over all physical space.

A pulse propagating in the PhC waveguide in the presence of the weak nonlinearity may be written as $E = \frac{1}{\sqrt{\epsilon}} \int dk A(k, t) |u, m, k\rangle$ where $A(k, t)$ is a time dependent coefficient of each k component. The k -space range over which the integrand is appreciable depends on the frequency distribution of the pulse. For pulses with $\frac{\Delta\omega}{\omega} \approx 10^{-6}$, and group velocity of $v = \frac{c}{100}$, $\frac{\Delta k}{k} \approx 10^{-4}$. So the integrand in the expression for E is dominated by a particular k about which the pulse can be expanded:

$$E = \int dk A(k, t) u_k(\vec{r}) e^{i(kz - \omega(k)t)} \approx u_{k_0}(\vec{r}) e^{i(k_0 z - \omega_0 t)} \int dk A(k, t) e^{i[(k-k_0)z - (\omega(k) - \omega_0)t]} \quad (5)$$

expanding $\omega(k) = \omega(k_0) + \frac{\partial\omega}{\partial k}|_{k=k_0}(k - k_0) + \frac{1}{2} \frac{\partial^2\omega}{\partial k^2}|_{k=k_0}(k - k_0)^2 = \omega_0 + v_g q + \frac{1}{2} \frac{\partial v_g}{\partial k} q^2$ with $q = k - k_0$ gives:

$$\begin{aligned} E &\approx u_{k_0}(\vec{r}) e^{i(k_0 z - \omega_0 t)} \int dq A(q + k_0, t) e^{i[q(z - v_g t) - \frac{1}{2} q^2 \frac{\partial v_g}{\partial k} t]} \\ &= u_{k_0}(\vec{r}) e^{i(k_0 z - \omega_0 t)} \times F(z, t) = \frac{1}{\sqrt{\epsilon}} |u, k_0\rangle \times F(z, t) \end{aligned} \quad (6)$$

Here F is a slowly spatially and time varying envelope of the signal or probe, which extends over many periods of the waveguide. In order to determine the interaction of pulses propagating in the PhC waveguide, we need to know the evolution of such an envelope. In the Appendix, first order perturbation theory is applied to the operator \hat{O} to determine the evolution of the Fourier components of the envelope. To first order in the nonlinear perturbation, and with negligible group velocity dispersion, the evolution of two pulses (S and P) in the same waveguide, but possibly coupled to different waveguide modes (s, p) is given by (see Appendix):

$$\dot{S} = i \frac{1}{2} \kappa \omega_s (\gamma_{s,s} |S|^2 + 2\gamma_{s,p} |P|^2) S - v_s S' + i \frac{1}{2} \frac{\partial v_s}{\partial k} S'' \quad (7)$$

$$\dot{P} = i \frac{1}{2} \kappa \omega_p (\gamma_{p,p} |P|^2 + 2\gamma_{p,s} |S|^2) P - v_p P' + i \frac{1}{2} \frac{\partial v_p}{\partial k} P'' \quad (8)$$

with:

$$\gamma_{s,p} = \frac{1}{a} \int_{\Lambda} d^3 r \tilde{\epsilon}(\vec{r}) |u_s|^2 |u_p|^2 \quad (9)$$

The dot in the above equation denotes differentiation in time, and the prime is a derivative in the direction of propagation (z). The overlap $\gamma_{s,p}$, has dimensions of m^{-2} , due to our re-normalization of the Bloch state to $\int_{\Lambda} d^3 r |u|^2 = a$. The function $\tilde{\epsilon}$ has a value of n^2 in the material and is zero in air. Here, p and s label the probe and signal modes at a particular k point, and v_s and v_p are the group velocities of the signal and probe pulses respectively; κ is defined as cn_2 (see Appendix). The intensity of each pulse is enhanced by $\frac{c}{v_{p,s}}$, relative to bulk, as can be shown from Poynting's theorem [15]. When there is no nonlinear coupling, each pulse propagates with group velocity $v_{s,(p)}$, and spreads according to $\frac{1}{2} \frac{\partial v_{s,(p)}}{\partial k}$. The above equations are derived in the Appendix and can be used to investigate self focusing, soliton formation, and other effects in PCW's. In the presence of the nonlinearity, the pulses experience self-phase modulation due to $\gamma_{s(p),s(p)}$ and cross-phase modulation due to $\gamma_{s,p}$ terms. The integral for $\gamma_{s,p}$, which gives the coupling strength, is taken over a unit cell of the waveguide, and is normalized by the length of the period a (see Appendix for further details).

The shape of u_s and u_p , and hence the values of the γ terms, is not strongly k dependent within numerical error for a wide range of wavevectors, as determined by 3D Finite Difference Time Domain (FDTD) simulations (Figure 2), and $\partial_k u_k \approx 0$. Thus, the coupling strength $\gamma_{s,p}$

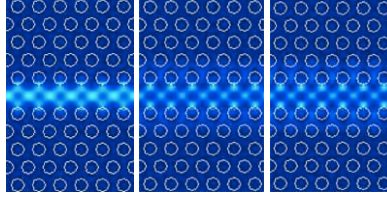


Fig. 2. Amplitude of E field for $k = \frac{2}{3} \frac{\pi}{a}$, $\frac{5}{6} \frac{\pi}{a}$ and $\frac{\pi}{a}$

only depends on the waveguide branch for the modes and not the particular k point. The total effective interaction strength is k dependent, since the group velocity determines the propagation time. The coupling strengths in units of a^{-2} , and mode volumes of the unit cell of the waveguide in units of a^{-3} , are shown in the Table 1. The mode volume for each waveguide mode is defined as $V_{1,1(2,2)} = (\epsilon |u_{1(2)}|^2)_{\max}^{-1} \int_{\Lambda} d^3r \epsilon |u_{1(2)}|^2$, and the mode volume for the overlap is $V_{1,2} = (\epsilon |u_1||u_2|)_{\max}^{-1} \int_{\Lambda} d^3r \epsilon |u_1||u_2|$.

Table 1. values for coupling γ for different modes of the waveguide in units of a^{-2} , and mode volumes for each unit cell of the waveguide (in units of a^{-3} . 1 and 2 refer to the first and second modes of the waveguide.

$u_{i,j}$	1, 1	2, 2	1, 2
$\gamma_{i,j}$	6.4×10^{-2}	7.9×10^{-2}	1.4×10^{-2}
V_{mode}	3.9×10^{-1}	2.8×10^{-1}	2.5×10^{-1}

Each equation can be transformed into a coordinate frame moving with the probe and signal respectively via $x = z - v_s t$ and $x = z - v_p t$. The dispersion terms in 7 complicate the solution. We will assume that the length of the waveguide is small enough so that the measurement of the induced phase and the measurement of the phase on the probe is unaffected by the dispersion throughout the propagation. With $\frac{\partial v_s}{\partial k}$ and $\frac{\partial v_p}{\partial k}$ neglected, the solution and upper bounds on the phases on the probe after time $t = \frac{L}{v_p}$ are:

$$P(z') = \text{Exp}[-i\kappa\omega_p \int_0^t (\gamma_{p,p}|P(z')|^2 + 2\gamma_{s,p}|S(z' + \Delta vt')|^2) dt'] P(0) = P(0)e^{i(\phi_P + \phi_S)} \quad (10)$$

$$\phi_P = \frac{1}{2} \kappa\omega_p \int_0^t \gamma_{p,p}|P(z')|^2 dt' \approx \frac{1}{2} \kappa\omega_p \gamma_{p,p} \frac{L}{v} |P(z')|^2 \quad (11)$$

$$\phi_S = \kappa\omega_p \int_0^t \gamma_{s,p}|S(z' + \Delta vt')|^2 dt' \approx \kappa\omega_p \gamma_{s,p} \frac{L}{v} |S(z')|^2 \quad (12)$$

3. Nonlinear Phase Shift

The phase ϕ_S is the phase on the probe due to the nonlinear interaction with the signal, and gives the signal photon number. In the appendix we derive that the ideal case of a negligible group velocity mismatch and a narrow probe, gives the phase shift per signal photon of:

$$\phi_{s,ideal} = cn_2 \gamma_{s,p} \hbar \omega_s \omega_p \frac{L}{v_p} \frac{1}{v_s \tau_s} \quad (13)$$

L is the length of the PhC and τ_s is the temporal width of the signal wavepacket.

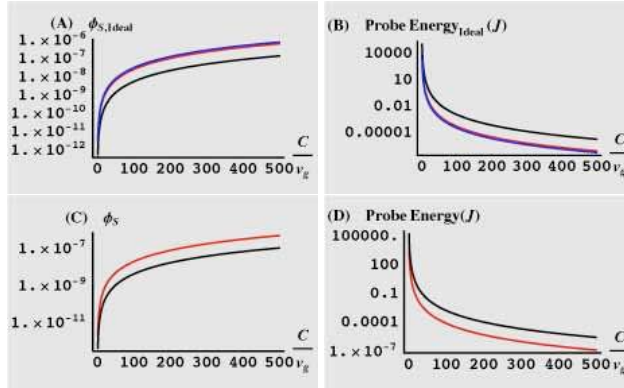


Fig. 3. Phase shift due to a single signal photon with a lifetime of 200 ps, after propagation through a $100\ \mu\text{m}$ AlGaAs waveguide with a narrow probe and no group velocity mismatch (A), and the energy required for an external pulse to obtain a SNR of 1 (B). In (A) and (B) it is assumed that the signal and probe are at 1500 nm and two-photon absorption is not present. In (C) we plot the phase for the case of the signal photon in waveguide 1 at 1550 nm and probe at 1620 nm in waveguide 0. The required probe energy for this scheme is shown in (D). In all plots, the blue and red curves correspond to both the signal and the probe in waveguide modes 0 or 1. The black curve corresponds to the probe and signal in different waveguide modes

Both the signal and probe wave undergo material absorption and scattering due to waveguide losses. PCW losses are already as low as $14\text{dB}/\text{cm}$ and will improve with time [16]. The material absorption consists of the linear absorption coefficient α_1 and the nonlinear coefficients, of which we will only consider the two photon absorption coefficient α_2 . In the case of AlGaAs at the half bandgap, the values of α_1 and α_2 were found to be $\approx .1\text{cm}^{-1}$ and $\approx .2\frac{\text{cm}}{\text{GW}}$ respectively [9]. Thus, α_1 limits us to $L\frac{c}{v_p} \approx 10\text{cm}$. For μJ and sub- μJ pulses, α_2 results in a smaller attenuation length on the order of $50\mu\text{m}$ at best. Thus, experiments with the signal and probe at the half-gap are not feasible. In order to circumvent pump depletion due to two photon absorption, a pump at even longer wavelengths above 1550 nm should be used [17]. In that case, α_2 is close to zero, and we will assume that the $100\ \mu\text{m}$ PCW length is the limit. In this case, the pump will propagate in the lower branch of the waveguide, while the signal should couple to the upper branch. For example for a signal at 1550 nm in the upper waveguide branch, a pump at 1620 nm should be used in order to have both beams velocity matched at the π/a point. We briefly mention that the GaInAsP material system has $\alpha_1 \approx 1\text{cm}^{-1}$, and $n_2 \approx 5 \times 10^{-12}\frac{\text{cm}^2}{\text{W}}$ and most likely similar two-photon absorption, which means that both materials are suitable candidates for an experiment. While the nonlinearity is enhanced closer to the band-edge of the semiconductor bandgap, the absorption increases accordingly and reduced the interaction length.

The phase due to a single photon in signal S and the energy required for an SNR of 1 for number state detection in AlGaAs, are plotted in Fig. 3. We plot both the ideal case, in which two-photon absorption is negligible, and the reality in which the pump is at 1620nm .

There are two sources of noise in this experiment in the case of an ideal detector. One is the phase noise due to intrinsic noise of the signal beam, and the other is the interferometer noise due to the uncertainty of the probe photon number. Following [12], it can be shown that in the case of a coherent signal state with mean photon number $\langle \hat{n}_s \rangle = N_s$ and coherent probe with mean photon number $\langle \hat{n}_p \rangle = N_p$ the uncertainty in the detected signal is $\langle \Delta n_{s,\text{observed}}^2 \rangle = \langle \Delta n_{s,\text{intrinsic}}^2 \rangle + \frac{\langle \Delta \hat{n}_p^2 \rangle}{\phi_s^2 N_p^2}$. There are two cases of interest: the signal in coherent and number states.

For the coherent state,

$$\frac{1}{\langle \Delta \hat{n}_{s,observed}^2 \rangle} = \frac{1}{N_s} + 4\phi_s^2 N_p \quad (14)$$

In the case of the signal in the number state, the intrinsic noise of the signal disappears,

$$\langle \Delta \hat{n}_{s,observed}^2 \rangle = \frac{1}{4\phi_s^2 N_p} \quad (15)$$

When the probe photon number is reasonably large, we can relax the requirement on N_p . If the tolerated error for coherent state detection is $E = \beta N_s$, then the condition is $N_p = (4\phi_s^2 \beta N_s)^{-1}$, and $\beta < 1$. Thus, detection of 1000 signal photons with an error of 100 ($\beta = 0.1$), would require $50 - 100nJ$. For smaller signal photon numbers, the level of tolerated error decreases, and the requirement is more stringent than number state detection, since $\frac{\beta}{N_s} > 1$.

4. Conclusion

In conclusion, we have derived the equations of motion for a probe and signal wave interacting via the third order nonlinearity in a photonic crystal waveguide. Within the slowly varying envelope approximation, the equations yield intuitive results, and are essentially identical to the equations of propagation for pulses in nonlinear fibers and materials, if the plane waves used in the mode expansion of the electromagnetic fields are replaced by Bloch waves. However, the user of PCW leads to the necessary enhancement of the pulse intensities due to the small mode volume and reduced group velocity of the pulses. We have shown that for the case of a very long wavelength probe pulse, that does not suffer from two-photon absorption in the AlGaAs material system, the energy requirement on the probe wave is within attainable values ($\approx \mu J$ in sub ns pulses). Since the sources of such pulses are external to the PCW, the generated probe pulse can be broader than the pulse desired in the PCW, due to contraction by the group velocity. Our derivation has assumed that coupling into the waveguides and the beamsplitter implementation in a PCW are perfect, and the scattering loss of the waveguide can be neglected. This is of course a gross generalization. High coupling efficiencies and low loss propagation over 10's of microns have been shown, and will only improve in time. We are in general most strongly limited by two photon absorption in this proposal. Other material systems such as GaInAsP [11], which also exhibit higher n_2 values than AlGaAs, could also be considered for this implementation, but ultimately atomic resonance systems and systems with a high phase shift and low loss are necessary [18, 19]. In principle, an on-chip QND photon number detector could be a component of a photonic crystal based quantum circuit, or can serve as a sensitive intensity detector and switch. The derivation presented here, can be easily extended to other types of intensity and field dependent nonlinearities, and can be used to analyze other nonlinear optical effects in PCW's, as well as soliton formation and propagation.

We would like to thank Dr. Edo Waks for his insight and help with the preparation of this manuscript. Financial support was provided by the MURI Center for photonic quantum information systems (ARO/ARDA Program DAAD19-03-1-0199) and the DARPA Nanophotonics seed grant. Ilya Fushman is supported by the NDSEG fellowship

5. Appendix

A. Derivation of the propagation equation

The probe envelope evolves according to (with $q = k - k_0$):

$$\begin{aligned}
\frac{\partial P}{\partial t} &= \frac{\partial}{\partial t} \int dk A(k, t) e^{i[(k-k_0)z - (\omega(k) - \omega_0)t]} \\
&\approx \frac{\partial}{\partial t} \int dq A(q + k_0, t) e^{i[q(z - v_g t) - \frac{1}{2} q^2 \frac{\partial v_g}{\partial k} t]} \\
&= \int dq \left(\frac{\partial A(q + k_0, t)}{\partial t} - i(v_g q + \frac{1}{2} \frac{\partial v_g}{\partial k} q^2) A(q + k_0, t) \right) e^{i[q(z - v_g t) - \frac{1}{2} q^2 \frac{\partial v_g}{\partial k} t]} \\
&= \int dq \frac{\partial A(q + k_0, t)}{\partial t} e^{i[q(z - v_g t) - \frac{1}{2} q^2 \frac{\partial v_g}{\partial k} t]} - (v_g \frac{\partial}{\partial z} - i \frac{1}{2} \frac{\partial v_g}{\partial k} \frac{\partial^2}{\partial z^2}) \int dq A(q + k_0, t) e^{i[q(z - v_g t) - \frac{1}{2} q^2 \frac{\partial v_g}{\partial k} t]} \\
&= \int dq \frac{\partial A(q + k_0, t)}{\partial t} e^{i[q(z - v_g t) - \frac{1}{2} q^2 \frac{\partial v_g}{\partial k} t]} - v_g \frac{\partial}{\partial z} P + i \frac{1}{2} \frac{\partial v_g}{\partial k} \frac{\partial^2}{\partial z^2} P
\end{aligned} \tag{16}$$

in the case of nonlinearity, the wave equation with $c^{-2} = \mu_0 \epsilon_0$ is:

$$-\nabla \times \nabla \times \vec{E} = \frac{1}{c^2} \frac{\partial^2 (\epsilon(\vec{r}) \vec{E})}{\partial t^2} + \mu_0 \frac{\partial^2 \vec{P}}{\partial t^2} \tag{17}$$

And we can rewrite this equation in terms of the previously introduced Hermitian field operator as:

$$-\frac{1}{\sqrt{\epsilon}} \nabla \times \nabla \times \frac{1}{\sqrt{\epsilon}} \sqrt{\epsilon} \vec{E} = -\hat{O} \sqrt{\epsilon} \vec{E} = \frac{1}{c^2} \frac{\partial^2 (\sqrt{\epsilon} \vec{E})}{\partial t^2} + \mu_0 \frac{\partial^2}{\partial t^2} \frac{1}{\sqrt{\epsilon}} \vec{P} \tag{18}$$

Here, in general, the polarizability P is given by $P_i = \epsilon_0 \sum_{j,k,l} \sum_{m,n,p} \chi_{i,j,k,l}^{(3)} E(\omega_p)_i E(\omega_s)_j E(\omega_p)_k$, where $\chi_{i,j,k,l}^{(3)}$ are the components of the third order nonlinearity tensor. In our case, we consider the system to be isotropic, the response instantaneous, and only two frequencies (ω_s, ω_p) to be present. To find the time evolution of the coefficients, we use the wave equation. In the presence of the nonlinearity we expand $\epsilon \approx \epsilon + \delta$ and \hat{O} as:

$$\begin{aligned}
\hat{O} + \Delta \hat{O} &= \frac{1}{\sqrt{\epsilon}} \nabla \times \nabla \times \frac{1}{\sqrt{\epsilon}} - \frac{1}{2} \left[\frac{\delta}{\epsilon} \frac{1}{\sqrt{\epsilon}} \nabla \times \nabla \times \frac{1}{\sqrt{\epsilon}} + \frac{1}{\sqrt{\epsilon}} \nabla \times \nabla \times \frac{1}{\sqrt{\epsilon}} \frac{\delta}{\epsilon} \right] + o \left[\left(\frac{\delta}{\epsilon} \right)^2 \right] \\
\hat{O} + \Delta \hat{O} &\approx \hat{O} - \frac{1}{2} \left[\frac{\delta}{\epsilon} \hat{O} + \hat{O} \frac{\delta}{\epsilon} \right] = \hat{O} - \frac{1}{2} \{ \frac{\delta}{\epsilon}, \hat{O} \}
\end{aligned} \tag{19}$$

Let $\langle u' | = \langle u, k', n' |$, $|u\rangle = |u, k, n\rangle$, $A = A(k, t)$. Then we have:

$$\begin{aligned}
\langle u' | (\hat{O} + \Delta \hat{O}) \int dk A |u\rangle &= -\langle u' | \frac{1}{c^2} \frac{\partial^2}{\partial t^2} \int dk A |u\rangle \\
\int dk A (\langle u' | \hat{O} |u\rangle + \langle u' | \Delta \hat{O} |u\rangle) &= -\langle u' | \frac{1}{c^2} \int dk (\ddot{A} - \omega^2 A - 2i\omega \dot{A}) |u\rangle \\
\int dk A \langle u' | \Delta \hat{O} |u\rangle &= \frac{2i\omega}{c^2} \int dk \dot{A} \langle u' |u\rangle \\
-\frac{1}{2} \int dk A \langle u' | \frac{\delta}{\epsilon} \hat{O} + \hat{O} \frac{\delta}{\epsilon} |u\rangle &= \frac{2i\omega}{c^2} \dot{A}(k') \\
-\frac{1}{2} \int dk A \langle u' | \frac{\delta}{\epsilon} |u\rangle \left(\frac{\omega'^2}{c^2} + \frac{\omega^2}{c^2} \right) &= \frac{2i\omega}{c^2} \dot{A}(k') \\
-\frac{\omega^2}{c^2} \int dk A(k) \langle u' | \frac{\delta}{\epsilon} |u\rangle &= \frac{2i\omega}{c^2} \dot{A}(k')
\end{aligned} \tag{20}$$

Above, we neglect second derivatives of the envelope and combine the two frequency terms as $\omega'^2 + \omega^2 \approx 2\omega^2 + v_s(k - k') \approx 2\omega^2$, because the $(k - k')$ term will lead to the derivative of the slowly varying envelope multiplied by the nonlinearity and is very small. Since the frequency bandwidth of the envelope is small, the envelope is slowly varying in time, and the second order time variation in the coefficients $A(k)$ is neglected. Furthermore, we have also assumed that the inner product $\langle u' |u\rangle$ is roughly unchanged by the nonlinearity – it remains a delta function. The

perturbation $\delta_{s,p}$ contains both the real and imaginary parts of the third order susceptibility. The real part is responsible for the cross phase modulation, while the nonlinear term gives the two photon absorption of the signal and probe. The figure of merit for the feasibility of the experiments is the phase-shift gained per loss length ($\frac{1}{e}$ point). The full perturbation can be written as:

$$\delta_{s,p} = i\alpha_1 + 3\epsilon_0(\chi_r^{(3)} + i\chi_i^{(3)})(|E(\omega_{s,p})|^2 + 2|E(\omega_{p,s})|^2) \quad (21)$$

Where $\chi^{(3)}$ is the third order polarizability (which is assumed to have only one value and to be infinitely fast), and $E(\omega_{s,p}) = \{S, P\}u_{k_{s,p}} e^{i(k_{s,p}z - \omega_{s,p}t)}$ is the electric field of the two modes. The linear loss α_1 is the imaginary part of the dielectric constant.

The value of $\chi_r^{(3)}$ can be determined from the experimentally observed bulk intensity dependent refractive index defined via $\tilde{n} = n + n_2I$, where I is the average field intensity. For a bulk material I is given by $I = \frac{1}{2} \sqrt{\frac{\epsilon_0 \tilde{\epsilon}}{\mu_0}} |E|^2 = \frac{1}{2} c \epsilon_0 n |E|^2$. Thus, $3\chi^{(3)} = cn^2 n_2$. For AlGaAs at the wavelength of $1.5 \mu m$, $n_2 \approx 1.5 \times 10^{-13} \frac{cm^2}{W}$; furthermore, the index is very similar for TE and TM polarization in AlGaAs slab waveguides [9]. Since $\chi^{(3)}$ measures the response of the local charge distribution to the local electric field, the coefficient itself is a material property and is not modified in the PCW, except possibly due to surface effects (e.g. reduced response or artificially added birefringence). Thus, we can derive the value of the coefficient from bulk experiments and combine it with the modified electromagnetic fields to get the resulting effect in the PCW. The $\chi^{(3)}$ coupling term only exists in the material, and we can replace the n^2 term with a dielectric which is equal to the spatially patterned index of AlGaAs in the PCW and is zero in the air. We set $3\chi^{(3)} = cn_2 \tilde{\epsilon}(\vec{r})$. And we define $\kappa = c\epsilon_0 n_2$, so that the perturbation due to real part of the nonlinearity becomes $\delta_{s,p} = \kappa \tilde{\epsilon}(\vec{r})(|E(\omega_{s,p})|^2 + 2|E(\omega_{p,s})|^2)$. The loss terms are similarly determined from a fit to $\alpha_{total} = \alpha_1 + \alpha_2 I$. The linear loss α_1 results in an exponential decay of the signal with a characteristic length $(\alpha_1)^{-1}$. The nonlinear loss gives a characteristic length of $(\alpha_2 I)^{-1}$. We will drop the losses for now, in order to derive the equation of motion for the pulses, and will assume that the Bloch components of the eigenstate $|u\rangle$ and $|u'\rangle$ belong to the same waveguide branch $n = n'$. Each of $u_{n,k}$, $u_{n,k'}$ is then roughly given by some central k component that is modulated by an envelope $u_{n,k} e^{ikz} \approx u_{n,k_0} e^{i(k_0 z - \omega_0 t)} e^{i[(k-k_0)z - (\omega(k) - \omega_0)t]}$. We now insert the exact form for $|u'\rangle$ and $|u\rangle$ into the above equation, and only look at the cross phase modulation component on the probe due to the signal. We take n to be branch of the pump mode p , and m to be that of the signal s , and only treat the perturbation due to the signal explicitly. Also, we will assume for simplicity that the signal group velocity v_s at k and k' , as well as the dispersion $\frac{\partial v_s}{\partial k}$, so that we can combine them in the expansion of the Bloch state. Eq. 20 then implies:

$$\begin{aligned} \dot{A}(k') &= i\omega_p \int dk'' \int d^3 r' A(k'') \kappa \tilde{\epsilon} |u_p|^2 |u_s|^2 |S(z')|^2 e^{i[(k''-k')z' - (\omega(k'') - \omega(k'))t]} \\ &\approx i\omega_p \kappa \int dk'' A(k'') \int dz' |S(z')|^2 e^{i[(k''-k')z' - (\omega(k'') - \omega(k'))t]} \frac{1}{\Lambda} \int_{\Lambda} d^3 r \tilde{\epsilon} |u_s|^2 |u_p|^2 \\ &\approx i\omega_p \kappa \gamma_{s,p} \int dk'' A(k'') \int dz' |S(z')|^2 e^{i[(k''-k')z' - (\omega(k'') - \omega(k'))t]} \end{aligned} \quad (22)$$

This is now inserted back into the evolution equation for the envelope 16, and we re-substitute $k - k_0 = q$ and keep the frequency term in the form $\omega(k) - \omega(k_0)$ for convenience.

$$\begin{aligned}
& \int dk \dot{A}(k, t) e^{i(k-k_0)z - (\omega(k) - \omega_0)t} = \\
& = i\omega_p \kappa \gamma_{s,p} \int dk \int dk'' A(k'') \int dz' |S(z')|^2 e^{i[(k''-k)z' - (\omega(k'') - \omega(k))t]} e^{i[(k-k_0)z - (\omega(k) - \omega_0)t]} \\
& = i\omega_p \kappa \gamma_{s,p} \int dz' \int dk'' A(k'') |S(z')|^2 e^{i[(k''z' - k_0z) - (\omega(k'') - \omega_0)t]} \int dk e^{ik(z-z')} \\
& = i\omega_p \kappa \gamma_{s,p} \int dz' |S(z')|^2 e^{ik_0(z'-z)} \delta(z-z') \int dk'' A(k'') e^{i[(k''-k_0)z' - (\omega(k'') - \omega_0)t]} \\
& = i\omega_p \kappa \gamma_{s,p} \int dz' |S(z')|^2 e^{ik_0(z'-z)} \delta(z-z') P(z') \\
& = i\omega_p \kappa \gamma_{s,p} |S(z)|^2 P(z)
\end{aligned} \tag{23}$$

The $\sqrt{\varepsilon}$ terms cancel the denominator of the perturbation. The term $\gamma_{s,p}$ contains an effective area integral $\gamma_{s,p} = \frac{1}{a} \int_{\Lambda} d^3 r \tilde{\varepsilon} |u_s|^2 |u_p|^2 \approx \int dx dy \tilde{\varepsilon} |u_s|^2 |u_p|^2$. Since the Bloch states are periodic, their integral in each unit cell ($\gamma_{s,p}$) is the same, and we simply weigh it by the average value of the slowly varying envelope in that cell to find the integral over the whole volume. Λ is the unit cell volume. S and P are only functions of time and the propagation coordinate (z here), and are uniform in the transverse (x, y) plane. The term κ contains the strength of the nonlinearity. We now re-normalize the Bloch state and the field:

$$N_s \hbar \omega_s = \int \int \int d^3 \vec{r} \varepsilon_0 \varepsilon(\vec{r}) |S|^2 |u_s|^2 \tag{24}$$

$$\approx \int dz \varepsilon_0 |S|^2 \frac{1}{a} \int_{\Lambda} d^3 \vec{r} \varepsilon(\vec{r}) |u_s|^2 \tag{25}$$

$$N_s \hbar \omega_s = \int dz \varepsilon_0 |S|^2 \tag{26}$$

$$1 = \frac{1}{a} \int_{\Lambda} d^3 \vec{r} \varepsilon(\vec{r}) |u_s|^2 \tag{27}$$

The above normalization means that $[\gamma] = m^{-2}$ and $[|S|^2] = \text{Vol}^2$. Thus the term $\kappa \gamma \omega |S|^2$ has units of s^{-1} , as desired. We now insert the form for \dot{A} into 16:

The refractive index due to cross-phase modulation is twice that of self phase modulation [8]. The evolution of the slowly varying envelope is given by:

$$\dot{S} = i \frac{1}{2} \kappa \omega_s (\gamma_{s,s} |S|^2 + 2\gamma_{s,p} |P|^2) S - v_s S' + i \frac{1}{2} \frac{\partial v_s}{\partial k} S'' \tag{28}$$

$$\dot{P} = i \frac{1}{2} \kappa \omega_p (\gamma_{p,p} |P|^2 + 2\gamma_{p,s} |S|^2) P - v_p P' + i \frac{1}{2} \frac{\partial v_p}{\partial k} P'' \tag{29}$$

We will now show the qualitative behavior of the two pulses, assuming a weak interaction. Take $P = \rho(z, t) e^{i\phi(z, t)}$ and $S = \eta(z, t) e^{i\psi(z, t)}$. Inserting P into 29, the real and imaginary parts satisfy:

Real:

$$\dot{\rho} + (v_p + \frac{\partial v_p}{\partial k} \phi') \rho' = -\frac{\partial v_p}{2} \phi'' \rho \tag{30}$$

Imaginary:

$$\dot{\phi} \rho + v_p \phi' \rho = \frac{1}{2} \kappa \omega_p (\gamma_{p,p} \rho^2 + 2\gamma_{s,p} \eta^2) \rho + \frac{\partial v_p}{2} (\rho'' - (\phi')^2 \rho) \tag{31}$$

If we assume that in 30 the second derivative term vanishes, then we can see that the envelope moves along a characteristic given by $v_p + \frac{\partial v_p}{\partial k} \phi' \approx v_p (k_0 + \phi')$, which, in the flatter regions of the dispersion curve is very close to $v_p(k_0)$. If $\frac{\partial v_p}{\partial k} (\frac{\rho''}{\rho}) \ll 1$, then 31 simplifies to give an

equation for the phase along a characteristic given by $v_p(k_0 + \frac{\phi'}{2})$.

$$\dot{\phi} + v_p \phi' + \frac{\partial v_p}{\partial k} (\phi')^2 = \frac{1}{2} \kappa \omega_p (\gamma_{p,p} \rho^2 + 2\gamma_{s,p} \eta^2) \quad (32)$$

Since we will not generally be able to generate a pulse that is a solution to the nonlinear system, we will assume that the pulses are Gaussian and drop the dispersion terms for simplicity of the analysis. We are essentially assuming that the envelopes are very slowly varying and that the interaction time and dispersion are not strong enough to affect the phase measurement, which is dominated by the group velocity term rather than the group velocity dispersion term. Thus, we will rewrite Eq. 29 in a frame moving with the group velocity in terms of $z' = z - v_p t$ and $t' = t$, and neglect the terms with $\frac{\partial v_p}{\partial k}$ and $\frac{\partial v_s}{\partial k}$. Since the two pulses may have different group velocities, we have $\Delta v = (v_p - v_s)$. If the group velocity dispersion terms are neglected, each envelope is only a function of z' .

$$\frac{dP(z')}{dt'} \approx \frac{i}{2} \kappa \omega_p (\gamma_{p,p} |P(z')|^2 + 2\gamma_{s,p} |S(z' + \Delta v t')|^2) P(z') \quad (33)$$

The solution, and upper bounds on the phases after time $t = \frac{L}{v_p}$ are:

$$P(z') = P(0) \text{Exp}[\frac{i}{2} \kappa \omega_p \int_0^t (\gamma_{p,p} |P(z')|^2 + 2\gamma_{s,p} |S(z' + \Delta v t')|^2) dt'] = P(0) e^{i(\phi_P + \phi_S)} \quad (34)$$

$$\phi_P = \frac{1}{2} \kappa \omega_p \int_0^t \gamma_{p,p} |P(z')|^2 dt' \approx \frac{1}{2} \kappa \omega_p \gamma_{p,p} \frac{L}{v_p} |P(z')|^2 \quad (35)$$

$$\phi_S = \kappa \omega_p \int_0^t \gamma_{s,p} |S(z' + \Delta v t')|^2 dt' \approx \kappa \omega_p \gamma_{s,p} \frac{L}{v_p} |S(z')|^2 \quad (36)$$

If the second arm of the interferometer is adjusted for a phase shift of $\pi/2$, the difference in the intensity signal on the two detectors gives the phase, and thus an estimate of the photon number. The total integrated signal energy is $I_{det} = \int \int \int d^3 r \epsilon_0 \epsilon |P(z')|^2 |u_n|^2 \sin(\phi_S)$. Starting from $N_s \hbar \omega_s = \int_{-\infty}^{\infty} dz' \epsilon_0 |S(z')|^2 = \int_{-\infty}^{\infty} dz' \epsilon_0 |S|^2 s(z')$ with $|S|^2 = \frac{N_s \hbar \omega_s}{\epsilon_0 L_{eff,S}}$ (similarly, $|P(z')|^2 = |P|^2 p(z')$ and $|P|^2 = \frac{N_p \hbar \omega_p}{\epsilon_0 L_{eff,P}}$), the integral for I_{det} is re-ordered again:

$$I_{det} \approx \int \int \int d^3 r \epsilon_0 |P(z')|^2 \phi_S(z') \epsilon |u_n|^2 \quad (37)$$

$$\approx \int dz' \epsilon_0 |P(z')|^2 \phi_S(z') \frac{1}{a} \int_{\Lambda} d^3 r \epsilon |u_p|^2 \quad (38)$$

$$= \int dz' \epsilon_0 |P(z')|^2 \phi_S(z') \quad (39)$$

$$\approx \kappa \omega_p \gamma_{s,p} \frac{L}{v_p} \frac{N_s \hbar \omega_s}{\epsilon_0 L_{eff,S}} \frac{N_p \hbar \omega_p}{L_{eff,P}} \int dz' p(z') s(z') \quad (40)$$

In the case when P is much narrower than the signal pulse S, we can view it as a quasi delta function $p(z') \approx L_{eff,P} \delta(x - x_0)$. The effective length can be approximated by the spatial width of the pulse, which is $\tau_s v_s$, the product of the temporal width and the group velocity of S. In this approximation the detected intensity is :

$$I_{det} \approx \kappa \omega_p \gamma_{p,s} \frac{L}{v_p} \frac{N_s \hbar \omega_s}{\epsilon_0 \tau_s v_s} N_p \hbar \omega_p \quad (41)$$

$$= c n_2 \hbar^2 \omega_p^2 \omega_s \gamma_{p,s} \frac{L}{v_p} \frac{N_s N_p}{\tau_s v_s} \quad (42)$$

And the phase shift per photon of S is $\frac{I_{det}}{N_p N_s \hbar \omega_p} = cn_2 \gamma_{p,s} \hbar \omega_s \omega_p \frac{L}{v_p} \frac{1}{v_s \tau_s}$. In order to make a comparison to our initial plane wave argument, we can identify $\gamma_{p,s}$ as the effective inverse area, $\frac{c}{v_s \tau_s}$ as the effective pulse bandwidth in the waveguide, and $\frac{L}{v_p}$ as the enhanced interaction length (time).

Acknowledgments

Financial support was provided by the MURI Center for photonic quantum information systems (ARO/DTO program No. DAAD19-03-1-0199) and the ONR Young Investigator Award. Ilya Fushman is supported by the NDSEG fellowship.